Chemical Engineering Journal 417 (2021) 129013

Contents lists available at ScienceDirect

Chemical Engineering Journal

journal homepage: www.elsevier.com/locate/cej

# Bimodal effect of water on $V_2O_5/TiO_2$ catalysts with different vanadium species in the simultaneous NO reduction and 1,2-dichlorobenzene oxidation

J.A. Martín-Martín, M. Gallastegi-Villa, M.P. González-Marcos, A. Aranzabal *, J. R. González-Velasco

*Group of Chemical Technologies for Environmental Sustainability, Department of Chemical Engineering, Faculty of Science and Technology, The University of the Basque Country, UPV/EHU, P.O. Box 644, E-48080 Bilbao, Spain*

ARTICLE INFO

*Keywords:*
Water effect
$VO_X/TiO_2$
$NH_3$-SCR
1,2-dichlorobenzene
Vanadium species
Deactivation

ABSTRACT

$VO_X/TiO_2$ catalysts with different vanadium loading were prepared in order to study the influence of vanadium species on the effect of water in the simultaneous NO reduction through $NH_3$-SCR and o-DCB oxidation reactions. The presence of isolated, polymeric and crystalline species and their redox and acid properties were evaluated by $N_2$-Adsorption, XRD, Raman, $H_2$-TPR, XPS and $NH_3$-TPD. Water has a bimodal and reversible effect in both NO reduction and o-DCB oxidation depending on vanadium species and temperature. In SCR, water has a detrimental effect at low temperature due to competitive adsorption with NO and $NH_3$, while at high temperature it promotes an increase of NO conversion associated to the suppression of side-reactions, which increase the selectivity towards $N_2$. In o-DCB oxidation, the effect of water is the sum of two contributions: one positive, related to the removal of surface adsorbed detrimental species; and one negative, associated to the competitive adsorption with o-DCB. Thus, at high temperature water acts as inhibitor, while at low temperature water has a promotional effect in the highly dispersed vanadium catalysts due to their tendency to suffer deactivation, mainly by carbonaceous materials. The presence of water also favors total oxidation and decreases the formation of chlorinated by products.

## 1. Introduction

Municipal solid waste incinerator (MSWI) plants are currently arising great controversy in society because of the wide diversity of pollutants generated in the combustion of municipal wastes, such as particulate matter, heavy metals, acid gases, nitrogen oxides ($NO_X$) and organic carbon compounds, as dioxin and Furans (PCDD/Fs), polycyclic aromatic hydrocarbons (PAHs) and halide volatile organic compounds (HVOC) [1–3]. For this reason, the flue gas clean (FGC) line is the most important part of these plants from the environmental point of view. $NO_X$ are usually abated applying the selective non catalytic reduction (SNCR), because it is relatively simple and cheap [4,5]. In SNCR, $NO_X$ are reduced to $N_2$ in the combustion chamber by injecting ammonia or ammonia precursors, such as urea [4,6–8]. The $NO_X$ efficiency in this process is approximately 40–70%, although ammonia excess conditions are necessary [7,9,10]. This fact usually causes an ammonia slip. Ammonia is a compound with high greenhouse effect, so additional systems must be installed in the FGC line to remove it. These levels of efficiency allow to reach the daily average $NO_X$ concentration sets in the Waste Incineration Directive 2000/76/EC [11]. However, emission legislations are moving towards tightening of pollutant emission limits, as it is in some regions of Germany [6]. In this context, Selective Catalytic Reduction (SCR) of $NO_X$ is a technology to consider, which has been implemented in many stationary sources including MSWI plants [9,10,12]. In this process, $NO_X$ reacts with $NH_3$ in a catalytic reactor with lower ammonia consumption and higher efficiency than SNCR [13].

On the other hand, several processes are reported in the literature to remove HVOC and specially PCDD/Fs [14–16]. Adsorption over activated carbon is the most commonly method used [15,17], although there are few references about other adsorbents, as hydrophobic zeolites and sepiolite [18,19]. Wet scrubbing with acid and basis sorbents is another alternative capable of reaching PCDD/Fs removal efficiencies of 98% [14]. However, both absorption and adsorption techniques only

* Corresponding author.
*E-mail address:* asier.aranzabal@ehu.eus (A. Aranzabal).

https://doi.org/10.1016/j.cej.2021.129013
Received 24 November 2020; Received in revised form 21 January 2021; Accepted 12 February 2021
Available online 24 February 2021

transfer the pollutants to other phases, which generates an additional waste that needs to be treated or disposed in a landfill. Alternatively, catalytic filter is an efficient abatement technology, which has been implemented in some MSWI to meet satisfactorily the required emission limits [20–22]. This technology allows to hold and destroy through catalytic oxidation reaction the PCDD/Fs from solid phase (adsorbed in dust) and gas phase. Hung et al [23] compared the chlorobenzenes and chlorophenols removal efficiencies of catalytic filters and the system composed by the injection of active carbon followed by bag filter. The former was more efficient than the latter, especially as the temperature was increased [23].

Catalytic oxidation of HVOCs and PCDD/Fs has been studied over different catalysts, such as novel metal-based catalysts, non-metal oxide catalysts and mixed metal oxide-based catalysts [24]. Several works have reported that SCR commercial catalyst, based on $V_2O_5/TiO_2$ formulation and doped with $MoO_3$ and/or $WoO_3$, is also active for PCDD/Fs catalytic oxidation [25,26]. This fact is the starting point of a process, in which both pollutants, $NO_X$ and PCDD/Fs, could be simultaneously removed through SCR and catalytic oxidation reactions in the same reactor. Few works deal with this issue. Wang et al [27] studied four sinter plants in Taiwan and reported lower dioxin concentrations in those plants in which the stack flue gas was treated with SCR. Moreover, Goemans et al [28] analyzed the simultaneous removal of $NO_X$ and PCDD/Fs in a SCR de$NO_X$ reactor in Ghent MSWI plant (Belgium), and reported 90 and 99% removal efficiency of $NO_X$ and PCDD/Fs, respectively. At laboratory scale, several works have studied the applicability of $VO_X/TiO_2$ formulation in the catalytic oxidation of PCDD/Fs [26,29–32], although many of them are performed with PCDD/Fs model compounds (chlorobenzene, o-dichlorobenzene, chlorophenol, etc.) and tested in the absence of $NO_X$ and $NH_3$. Thus, additional experiments are necessary to understand the behavior of both reactions, SCR and PCDD/Fs catalytic oxidations, when they are performed simultaneously.

The use of de$NO_X$ unit to remove PCDD/Fs is reported in the Best Available Techniques (BAT) Reference Document for Waste Incineration, as a technique for the reduction of emission of organic carbon compounds, together with the $NO_X$ [10]. This combined abatement process would lead to significant cost savings for the future MSWI plants, because two pollutants, that are currently removed separately, would be threaten simultaneously in the same catalytic bed. However, according to BAT reference document, the implementation of this technology is linked to the development of more efficient SCR systems than those used only for de$NO_X$ function. This fact inevitably involves the need of further research about catalytic properties that maximize the removal of both pollutants in the same range of temperature.

$V_2O_5/TiO_2$ catalysts may present different $VO_X$ species depending on vanadium surface density. Monomeric and polymeric species are formed at surface vanadium concentration below monolayer coverage. The main difference between both is that polymeric species present more V-O-V bonds. On the contrary, vanadium surface density above monolayer coverage promotes the formation of $V_2O_5$ crystalline species [33]. The role of vanadium species in SCR and oxidation of chlorinated compounds has been investigated in several works. In SCR reaction, Amiridis et al. [34] proposed that turn-over frequency (TOF) reached a maximum at approximately half the monolayer coverage, because higher vanadium surface concentration causes a decrease of strong acidity. On the other hand, there is disagreement about the optimum combination of vanadium species for the oxidation of chlorinated benzenes. Krishnamoorthy et al. [35] supported that high conversion of 1,2-dichlorobenzene is obtained with vanadium surface coverage below the monolayer, although they also found that TOF is independent of vanadium coverage. Delaigle et al. [36] concluded that the best catalytic performance is achieved with highly dispersed, amorphous vanadium species. On the contrary, Schimmoeller et al. [37] evidenced a decrease of catalytic activity with isolated vanadium species, catalysts with high amount of V-O-V bonds (amorphous polymeric and/or crystalline $VO_X$) showing a superior activity.

Operating conditions also play an important role in efficiency and stability of the catalytic systems. In this regard, the SCR unit in MSWI plants may operate in different way depending FGC line configuration. There are three typical location for de$NO_X$ unit: in high-dust position, the SCR reactor is placed upstream of the particulate removal devices. It is a very common configuration despite catalyst can easily degraded by ash erosion and chemical poisoning; in low-dust position, the SCR reactor is placed downstream of the dust and particle removal. This configuration requires a flue gas reheating system to maintain the optimum operating temperature; in tail-end position, the SCR reactor is placed downstream of the particulate removal devices and flue gas desulfurization and acid removal, just before the stack. Although costly gas reheat is also necessary, tail-end is the most common configuration in MSWI plants because it avoids the poisoning of the catalyst.

Regardless of the type of configuration, there are some components in exhaust gases, as water, that may affect to catalytic efficiency. Water, usually in a concentration of 10–20 vol% in MSWI plants [10], may interact with the catalysts changing the distribution of Lewis and Brønsted acid sites. Thus, water affects the interaction between reactants and active sites, modifying reaction kinetics and even catalyst durability. According to literature, the majority of research agrees that water inhibits SCR reactions, although Huang et al. [38] reported that inhibition increases with water content, whereas Wach et al. [33] proposed that detrimental effects do not increase at water concentrations above 5%. On the other hand, there are same discrepancies about the effect of water in chlorobenzenes oxidation. A promoting effect was observed in the oxidation of 2,4,6-trichlorophenol over V-based catalysts [29] and in the oxidation of dichlorobenzene over perovskites [39], whereas a detrimental effect was reported by Albonetti et al. [40] in o-DCB conversion over $V_2O_5/WO_3$ based catalysts. These conclusions correspond to works in which the SCR of NO and the oxidation of chlorinated benzenes were analyzed separately. Recently, it has been found that NO reduction and o-DCB oxidation rates differ when they are performed simultaneously [41,42] in dry conditions. However, there is no data in the literature about the effect of water on the catalytic behavior of simultaneous abatement of NO and chlorinated benzenes over different $VO_X$ species in $V_2O_5/TiO_2$ catalyst [44,45].

Then, in the present work, $V_2O_5/TiO_2$ catalysts with different vanadium coverage were prepared in order to determine the effect of water in the simultaneous abatement of NO and o-DCB over catalysts with different distribution of vanadium species.

## 2. Experimental

### 2.1. Catalyst preparation

The $VO_X/TiO_2$ samples were prepared by wet impregnation, fixing the vanadium loading in 1, 3 and 8 wt% in order to obtain catalysts with vanadium surface density corresponding to sub-monolayer, monolayer and over-monolayer catalysts, respectively. $NH_4VO_3$ (Sigma Aldrich, 99.99%) was used as precursor of vanadium species, which was dissolved in distilled water and complexed with 2 mol of oxalic acid (Sigma-Aldrich, 99.99%) per mol of vanadium. Commercial $TiO_2$ anatase (from Millennium Inorganic Chemicals-Cristal Global (Cristal ACTiVTM G5) calcined at 550 °C for 3 h was used as support. The solution slurry resulting from the mix of precursor solution and support was kept in contact in continuous stirring for 1 h using a rotary evaporator. The solvent evaporation was done in vacuum and 40 °C. The solid samples obtained were dried overnight at 110 °C and calcined at 500 °C for 3 h with a heating rate of 1 °C/min. Finally, the solids were pelletized, crushed and sieved to 0.3–0.5 mm. The catalysts were named as 1 $V/TiO_2$, 3 $V/TiO_2$ and 8 $V/TiO_2$, where the number indicates the mass percentage of vanadium in each catalyst.

### 2.2. Catalyst characterization

V and Ti content in the catalysts was measured by XRF. The measurements were conducted in a dispersive X-ray fluorescence spectrometer (WDXRF, PANalytical, AXIOS model) with a Rh tube. The fused beads for analysis were produced by mixing a flux (Spectromelt A12, Merck) with the samples (ratio 20:1) that were finely powdered and then heated to temperature between 1000 °C and 1200 °C.

$N_2$ adsorption–desorption experiments at liquid nitrogen boiling temperature were performed to evaluate the textural properties of the samples using a Micromeritics TRISTAR II 3020. Prior to the experiments, the samples were pre-treated at 350 °C with $N_2$ to remove the physisorbed species over the catalytic surface. BET surface area and pore average size were calculated using the BET procedure (adsorption branch in 0.03–0.3 equilibrium pressure range) and BJH method (desorption branch), respectively.

Redox properties were studied by temperature programmed reduction with $H_2$ ($H_2$-TPR) in a Micromeritics AutoChem 2920. Firstly, a pretreatment of the samples was carried out at 500 °C with a 5% $O_2$/He stream. Afterwards, the samples were cooled down to 100 °C, the started temperature of the experiments. Finally, the experiments were performed passing a 5% $H_2$/Ar stream through the sample and increasing the temperature to 900 °C using a rate of 10 °C/min. A TCD detector was used for monitoring the $H_2$ consumption. The water produced during the experiments was trapped in a cold trap.

Catalysts surface acidity was studied by temperature programmed desorption of ammonia ($NH_3$-TPD) and by FTIR analysis of adsorbed $NH_3$ ($NH_3$-IR). $NH_3$-TPD experiments were performed on a Micromeritics AutoChem 2920 instrument. The catalytic samples were fully oxidized at 500 °C with a 5% $O_2$/He stream and then, cooled down to 50 °C. Then, $NH_3$ was adsorbed to saturation by flowing a 1% $NH_3$/He stream (130 mL/min) through the catalysts. Physisorbed $NH_3$ in the surface was removed with a helium flow for 60 min. $NH_3$ desorption was promoted by the temperature increase of the samples up to 500 ºC using a rate of 10 °C/min and a helium flow as carrier. $NH_3$ desorption was measured with a TCD detector. $NH_3$-IR was performed in an Agilent Cary 600 Series FTIR Spectrometer. The spectra were collected by 50 scans with a resolution of 4 $cm^{-1}$. Previously, the powdered samples compressed into a disc were pre-treated under 5% $O_2$/Ar stream at 480 °C for 30 min. Next, $NH_3$ adsorption was carried out by continuous feeding of a 1000 ppm $NH_3$/Ar stream during 30 min at 100 °C. Finally, physisorbed $NH_3$ was evacuated with an Ar stream during 30 min. In order to analyze the stability of chemisorbed $NH_3$, spectra at 100, 200, 300 and 400 °C were recorded.

The crystal phases of the catalysts were analyzed by X-ray diffraction (XRD), by comparing the difractogram with the JCPDS database. A Philips PW 1710 X-ray diffractometer with Cu Kα radiation ($\lambda = 1.5406$ Å) and Ni filter was used to perform the measurements with 0.026° per second sampling interval.

Raman spectroscopy was used in order to characterize the vanadium species at low vanadium coverages. The spectrometer device was a Renishaw System 1000 with a 706 nm solid-state laser as excitation line, which supplied a power of 1 mW on the sample. The sample powder was analyzed in the spectral window from 250 to 1200, using 20 s per scan and accumulating 5 scan per catalyst. The analysis was performed at 400 °C after dehydrating the samples at 400 °C for 3 h.

X-ray Photoelectron Spectroscopy (XPS) was carried out in a SPECS system with a monochromatic radiation source Al Kα (1486.6 eV). A Phoibos 150 1D-DLD detector was used. The analysis was performed with a pass energy of 30 eV, step energy of 0.08, dwell time of 0.1 and with a 90° electron exit angle.

Elemental analyses of used catalysts under dry and wet condition were conducted in a Carl Zeiss EVO 40 equipped with an EDS detector (Oxford Instrument X-Max). The measurements were made at approximately 10 nm with 20 kV and 100–400 pA.

### 2.3. Reaction set-up and catalytic tests.

The feedstream to the catalytic reactor was composed by $O_2$ (10%), NO (300 ppm), $NH_3$ (300 ppm), o-DCB (100 ppm) and Ar to balance. The concentrations of the components were selected with the aim to reproduce the actual composition of the gas stream at the inlet of the catalytic reactor in a tail-end configuration of the MSW incineration plant flue gas cleanup system. CO and $CO_2$ are also present at the outlet gas stream of MSW incineration plants, although they were not included because we have already checked they do not significantly affect NO reduction nor o-DCB oxidation, and because their excess makes it difficult to analyze the selectivity towards them. Water was only present in the experiments when its effect was studied, because when combined with reaction products it can damage pipes and gas analyzers by corrosion. Finally, o-DCB was used instead of PCDD/Fs, due to the difficulty of handling such toxic components.

Reactor feed composition was adjusted by mixing pure components, whose flow was regulated by mass flow controllers for gases (Bronkhorst® High-Tech F-201CV) and liquids (Bronkhorst® High-Tech μ-Flow *L*01-AAA-99–0-20S). Complete evaporation of the liquid stream and homogeneous mix with the gas stream was performed in a controlled-evaporator-mixer (Bronkhorst® High-Tech W-102A-111-K). In order to avoid gas adsorption and condensation, the pipes were heated with electrical resistances.

A tubular quartz reactor (13.6 mm internal diameter) inside a convective-flow oven was used. Gas stream went downflow. The catalytic bed was composed by 1.5 g of 0.3–0.5 mm sieved catalyst diluted with quartz in order to ensure a reactor volume of 3 $cm^3$ and a GHSV value of 60,000 $h^{-1}$. Before catalytic test, the fixed bed was pre-treated at 200 °C for 2 h with pure argon flow (2 $L_N$/min).

An ABB Limas analyzer was used to measure continuously the $NH_3$ $NO_2$ and NO concentrations, and an ABB Uras 26 infrared analyzer was used to measure the $N_2O$, $CO_2$ and CO concentrations. The o-DCB concentration and chlorinated byproduct compounds were measured by GC/MS (Agilent 7890A gas chromatograph with a HP-VOC capillary column and Agilent 5975C mass detector). $NH_3$ was not measured because the interference of o-DCB in the ABB Limas 21 analyzer. A process flow diagram is shown elsewhere [43].

Two types of experiments were carried out to analyze the effect of water. On the one hand, the fixed bed of catalyst, fed at a constant flow rate (2 $L_N$/min at 1.5 atm), was submitted to a 1.5 °C/min rise in temperature from 100 to 500 °C. These experiments allowed to compare the

**Table 1**
$VO_x/TiO_2$ catalysts characterization results.

| Sample | V(wt. %) | V($VO_x$/$nm^2$) | $S_{BET}$($m^2$/g) | $V_p$($cm^3$/g) | Anatase crystal size (nm) | $H_2$ consumption(mmol $H_2$/g) | $H_2$/V | Acidity(μmol $NH_3$/g) | Acidity(μmol $NH_3$/$m^2$) |
|---|---|---|---|---|---|---|---|---|---|
| $TiO_2$ | – | – | 69.3 | 0.24 | 20.5 | 0.25 | – | 349.7 | 5.0 |
| 1 V/$TiO_2$ | 0.86 | 1.45 | 58.9 | 0.24 | 19.4 | 0.48 | 1.4 | 360.9 | 6.1 |
| 3 V/$TiO_2$ | 2.92 | 4.93 | 52.4 | 0.22 | 22.1 | 0.81 | 1.0 | 330.6 | 6.3 |
| 8 V/$TiO_2$ | 8.14 | 13.16 | 31.5 | 0.18 | 24.7 | 1.83 | 1.0 | 200.6 | 6.4 |

typical light-off curves for NO and o-DCB conversion in the absence and in the presence of water (0.5%). On the other hand, the fixed bed of catalyst in isothermal conditions was submitted to cycles of dry–wet–dry atmosphere through a step change in flow of water vapor over the continuous flow of the dry feedstream, so that water concentrations were increased in two consecutive steps to 0.5% and 2%. Finally, the water flow was stopped to restore the initial dry conditions. Each step lasted for 100 min. The experiments were run at 150, 250 and 350 °C and conversion and products outlet concentration were monitored as a function of time-on-stream (TOS).

NO and o-DCB conversion were calculated from Eq. (1) and (2), respectively. Selectivity to $CO_2$ and CO was calculated through Eq. (3) and (4), respectively.

$$X_{NO} = \frac{C_{NO,in} - C_{NO,out}}{C_{NO,in}} \cdot 100 \quad (1)$$

$$X_{oDCB} = \frac{C_{o-DCB,in} - C_{o-DCB,out}}{C_{o-DCB,in}} \cdot 100 \quad (2)$$

$$S_{CO_2} = \frac{C_{co_2,out}}{6 \cdot (C_{o-DCB,in} - C_{o-DCB,out})} \cdot 100 \quad (3)$$

$$S_{CO} = \frac{C_{co,out}}{6 \cdot (C_{o-DCB,in} - C_{o-DCB,out})} \cdot 100 \quad (4)$$

## 3. Results and discussion

### 3.1. Catalyst characterization

Chemical composition, textural and structural properties of catalysts are summarized in Table 1. Vanadium loading, obtained by XRF, is close to the nominal values. Table 1 also includes the estimated vanadium dispersion as surface density ($VO_X/nm^2$), calculated from vanadium loading and BET surface area of $TiO_2$ support. 1 V/$TiO_2$ catalyst clearly shows sub-monolayer coverage because its surface density is much lower than theoretical monolayer value, which is ranging between 5.5 and 8 $VO_X/nm^2$ [46]. Higher vanadium content increases surface density of the catalysts, leading to values close to the monolayer in 3 V/$TiO_2$ and over-monolayer in 8 V/$TiO_2$ catalysts.

$N_2$ physisorption at –196 °C of pure $TiO_2$ and $VO_X/TiO_2$ catalysts show type IV isotherms (Fig. 1), associated to mesoporous solids

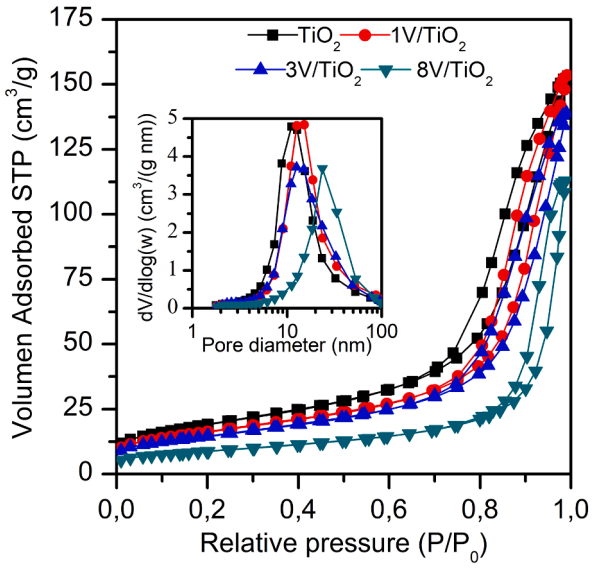


**Fig. 1.** $N_2$ adsorption–desorption isotherms and pore size distribution of $VO_X/TiO_2$ catalysts.

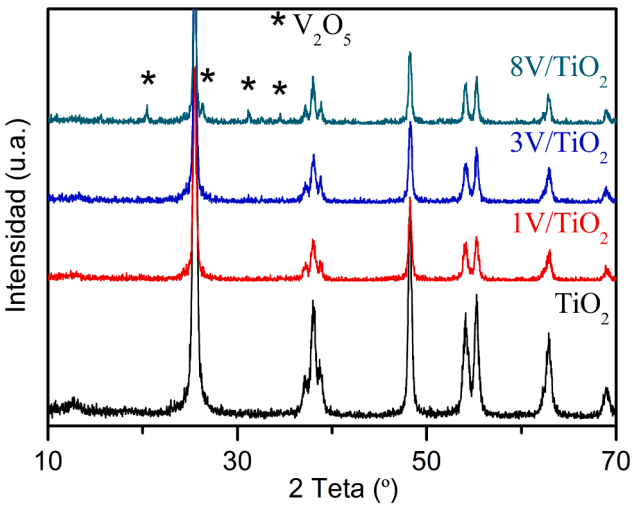


**Fig. 2.** XRD patterns of $VO_X/TiO_2$ catalysts.

according to IUPAC classification. BET surface areas and pore volumes are listed in Table 1. The increase of vanadium loading produces a decrease of BET surface area from 69 $m^2/g$ for pure $TiO_2$ to 32 $m^2/g$ for 8 V/$TiO_2$ [40] and pore volume. Moreover, Fig. 1 shows the pore size distribution of catalysts. No great differences have been found between pure $TiO_2$, 1 V/$TiO_2$ and 3 V/$TiO_2$. However, pore size of 8 V/$TiO_2$ catalyst became larger, which is probably associated to high vanadium contents favors the formation of $TiO_2$ aggregates. This fact promotes larger pore sizes [47].

XRD patterns of catalysts are shown in Fig. 2. All diffractograms show the presence of characteristic peaks attributed to $TiO_2$ anatase crystal phase (JCPDS 71–1272). Anatase crystalline size, calculated by Scherrer equation, increases with vanadium loading (Table 1). In samples 3 V/$TiO_2$ (22 nm) and 8 V/$TiO_2$ (25 nm), crystal size is even larger than in pure $TiO_2$ (20 nm). A similar behavior was observed in the literature [41]. According to $N_2$ physisorption results, a decrease of pore volume and surface area was observed at higher vanadium loading (Table 1). These results suggest a partial loss of the porosity support, caused by the vanadium deposition in the interphase of $TiO_2$ particles. The location of this vanadium elements in the $TiO_2$ interphase could cause a solid state diffusion (sintering of $TiO_2$ crystal domain) and larger $TiO_2$ crystal sizes would be promoted.

Vanadium crystalline species are not detected, except in sample 8 V/$TiO_2$, because their crystalline domain sizes are below 5 nm, which becomes difficult to analyze by XRD. This result suggests that vanadium is highly dispersed over the support and/or is part of amorphous structures. In sample 8 V/$TiO_2$, peaks associated to $V_2O_5$ (JCPDS 001–0359) appear at 20.4, 26.3, 31.2 and 34.5°. This result reveals that the formation of $V_2O_5$ crystals is promoted on over-monolayer vanadium surface coverage.

Raman spectroscopy is sensitive to dispersed and crystalline vanadium species and it was also used to characterize the structure of vanadium species. Raman spectra of dehydrated catalysts are shown in Fig. 3. All $VO_X/TiO_2$ samples show a band at 1026–1030 $cm^{-1}$ associated to the vibration of the terminal bond V = O. This band is shifted from 1026 to 1030 $cm^{-1}$ at higher vanadium loading because of vibrational coupling of adjacent V = O bonds consequence of $VO_X$ surface polymerization [48,49]. The increase of vanadium loading above 3 wt% promotes the appearance of a broad band at 940 $cm^{-1}$ related to the vibration of V-O-V bonds [37,49,50], which indicates the polymerization of isolated $VO_X$ species. The sharp band at 991 $cm^{-1}$ in 8 V/$TiO_2$ catalyst is associated to vibration mode of crystalline $V_2O_5$ [51], which is in accordance with the $V_2O_5$ crystal peaks observed in the XRD pattern of 8 V/$TiO_2$. Moreover, $VO_X/TiO_2$ catalysts also show a broad band at approximately 792 $cm^{-1}$, which is also present in pure $TiO_2$. This band is

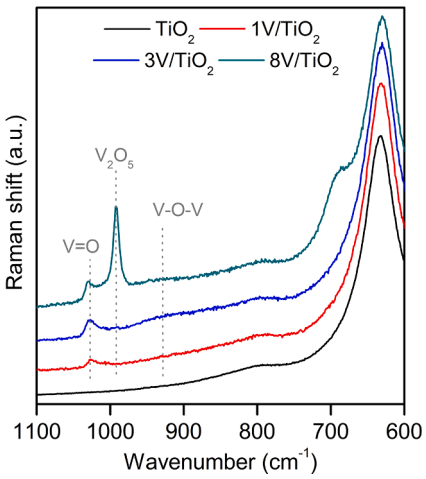


**Fig. 3.** Raman spectra of $VO_X/TiO_2$ catalysts.

associated to overtone vibration of crystalline anatase [48].

Therefore, the above results corroborate the formation of different surface vanadium species depending on vanadium surface density. Low vanadium coverage (1 V/$TiO_2$, 1.45 V atoms/$nm^2$) favors the formation of isolated vanadium species, which are polymerized by the increase of vanadium loading (3 V/$TiO_2$, 4.93 V atoms/$nm^2$). These conclusions are in accordance with Lai et al. [33], who reported 2–8 V atoms/$nm^2$ as the vanadium surface density in which isolated $VO_X$ species polymerize through V-O-V bonds. Surface vanadium densities above monolayer coverage (8 V/$TiO_2$, 13.16 V atoms/$nm^2$) lead to the formation of crystalline $V_2O_5$, consequence of the vanadium superposition over the monolayer.

Redox properties of pure $TiO_2$ and $VO_X/TiO_2$ catalysts were studied by $H_2$-TPR and the results are shown in Fig. 4. $TiO_2$ profile shows a peak at 540 °C, which may be associated to $TiO_2$ surface reduction [52]. Reduction of $VO_X/TiO_2$ catalysts takes place in a single reduction step, which occurs at higher temperature as the vanadium loading is increased. The reduction peaks are located at 417, 439 and 515 °C for 1, 3 and 8 wt% vanadium, respectively. The shift of the reduction peaks at different vanadium loading suggests a relation between the reducibility of the samples and the degree of surface vanadium polymerization, that is, the vanadium species. The decrease of reduction temperature at lower vanadium loading is associated to the increase of the interaction between vanadium atoms and the support, promoted by the higher

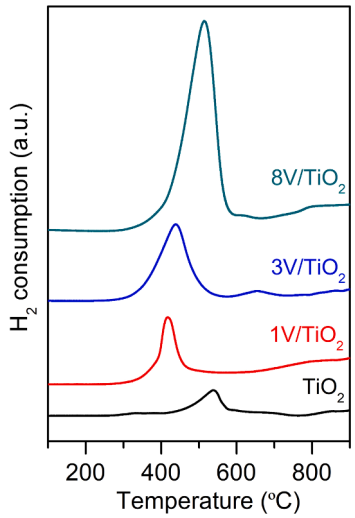


**Fig. 4.** $H_2$–TPR profiles of $VO_X/TiO_2$ catalysts.

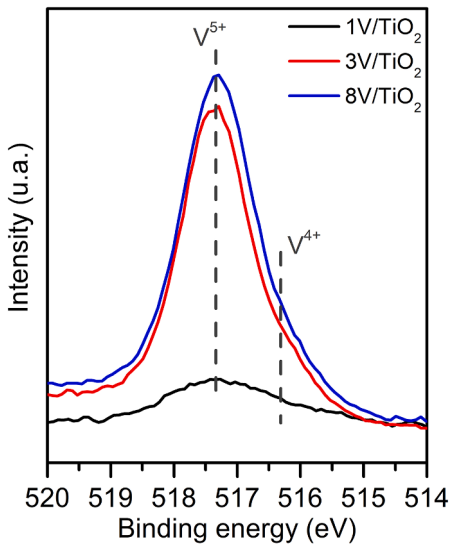


**Fig. 5.** V 2p 2/3 XPS spectra of $VO_X/TiO_2$ catalysts.

active phase dispersion [41,53].

Table 1 shows the quantification of $H_2$ consumed in each reduction peak of Fig. 4. It was calculated by time-integration of TPR profiles. These values allow the calculation of $H_2$/V ratio, so as to estimate the vanadium oxidation state average in each sample. $H_2$/V ratio of 3 V/$TiO_2$ and 8 V/$TiO_2$ is 1, which suggests that the single reduction peak is associated to vanadium reduction from $V^{5+}$ to $V^{3+}$. In the case of 1 V/$TiO_2$ catalyst, $H_2$/V ratio is higher than 1, which could be related to the reduction of surface oxygen and hydroxyl groups of surface $TiO_2$, influenced by the high vanadium dispersion [41].

XPS technique was used to know the oxidation state of surface vanadium, because slight differences in vanadium oxidation state may exist between bulk and surface vanadium, due to the different environment of each.

The V 2p 3/2 of each catalyst is shown in the Fig. 5. Binding energies are reference to C 1 s spectrum at 284.5 eV. All the spectra show a peak centered at 517.3 eV, whose relative intensity increase with vanadium loading. Moreover, all samples show an additional contribution around 516.3 eV, which became more relevant in the 1 V/$TiO_2$ catalyst. According to literature, the bands located around 517–518 eV and 516–516.5 eV are associated to $V^{5+}$ and $V^{4+}$ oxidation state, respectively [54–56]. Therefore, these results evidence $V^{5+}$ as the main oxidation state in all catalysts, which is in accordance with TPR results. However, small amount of surface $V^{4+}$ species are also present becoming more prominent at lower vanadium loading. Similar results were reported by S. Youn et al, who observed a promotion of $V^{4+}$ oxidation state in $VO_X/TiO_2$ catalysts with high vanadium dispersion [57].

The role of the $VO_X$ species on acidity, which is associated to the activation of reactants over the catalytic surface, was analyzed through two different experiments based on $NH_3$ adsorption over the samples: $NH_3$-IR and $NH_3$-TPD. The former allows the characterization of the nature of the acid sites (Lewis or Brønsted) and the latter gives information about the strength and the amount of acid sites. Thus, $NH_3$ desorption at low temperature is associated to $NH_3$ weakly adsorbed on the catalysts, whereas peaks at high temperature are attributed to $NH_3$ species adsorbed over strong acid sites.

Quantitative results, summarized in Table 1, show an increase of total acidity of the 1 V/$TiO_2$ catalyst with respect to the bare support. However, the increase of vanadium loading produces a gradual decrease of total acidity. Table 1 also shows the total acidity per unit area. In this case, the increase of vanadium loading promotes higher acidity per surface area, which suggests that the decrease of total acidity observed per mass of catalyst is probably related to the decrease of surface area at

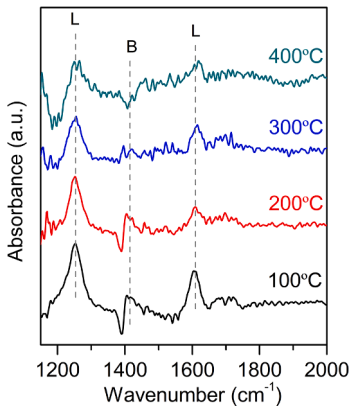


**Fig. 6.** FTIR results of adsorbed $NH_3$ in 3 $V/TiO_2$ catalyst at different temperatures.

higher vanadium loading.

Fig. 6 shows the $NH_3$-IR spectra of 3 $V/TiO_2$ catalyst at different temperatures. The adsorption of $NH_3$ clearly produces the appearance of three bands. The bands located at 1250 and 1613 $cm^{-1}$ are associated to N–H vibration mode of $NH_3$ adsorbed over Lewis acid sites, whereas the band at 1419 $cm^{-1}$ is related to N–H vibration of $NH_3$ adsorbed over Brønsted acid sites [58,59]. Therefore, these results suggest that $VO_X/TiO_2$ catalysts have both Lewis and Brønsted acid sites. However, the temperature increase causes a decrease in the intensity of the $NH_3$ adsorbed over Brønsted acid sites in comparison with the bands related to $NH_3$ adsorbed over Lewis acid sites. Then, acidic strength of Brønsted acid sites is weaker.

$NH_3$-TPD profiles are shown in Fig. 7. Desorption profile of $TiO_2$ is characterized by a broad desorption peak at relatively low temperature, around 130 °C, followed by a progressive decrease of $NH_3$ desorption at higher temperatures. This profile indicates that $TiO_2$ has a wide but mostly weak acid strength distribution. The addition of supported $VO_X$ provides an increase of medium and strong acidity. The lowest vanadium loading catalyst (1 $V/TiO_2$) shows a well-defined peak at 405 °C, which does not exist for higher vanadium loading samples (3 $V/TiO_2$ and 8 $V/TiO_2$). However, the profile of these catalysts shows a desorption shoulder around 255 °C, corresponding to medium strength acidity·$NH_3$-IR analysis revealed that adsorbed $NH_3$ is more stable over Lewis acid sites due to a stronger interaction with the catalyst. This result suggests that $NH_3$ desorption at high temperature in 1 $V/TiO_2$ catalyst may be associated with Lewis acid sites and, therefore, this type of acidity is only observed in highly dispersed monomeric species. On the contrary, the acidity of polymeric species is weaker and mostly contributed by Brønsted acidity. Similar results were observed by

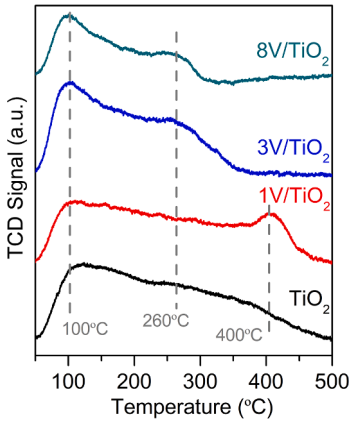


**Fig. 7.** $NH_3$-TPD profiles of $VO_X/TiO_2$ catalysts.

Gallastegi et al. [42], who proposed that Brønsted acidity of $VO_X$ could be related to oxygen bridge in V-O-V, characteristic of polymeric and crystalline vanadium species.

To sum up, the results of characterization analysis have evidenced the formation of different $VO_X$ species depending on surface vanadium coverage. Monomeric or highly isolated species are promoted at low vanadium coverage, as in 1 $V/TiO_2$ catalyst. Further increase of vanadium loading leads to the formation polymeric and crystalline species. The polymerization of monomeric species has been evidenced by Raman through the appearance of the broad band associated to V-O-V in the 3 $V/TiO_2$ catalyst, whereas crystalline species have been detected by both Raman and XRD, as consequence of the growing of $V_2O_5$ crystals.

$H_2$-TPR results have been also useful to corroborate the presence of the different vanadium species due to the different reduction temperatures of each catalyst. This fact denotes different redox properties depending on vanadium surface coverage. In this sense, monomeric species are characterized by a high degree of isolation that involves a high interaction between vanadium and support through V-O-Ti bonds, which makes the reduction of vanadium easier, in contrast to polymeric and crystalline species where V-O-V bonds are predominant.

### 3.2. Catalytic performance in dry conditions

The light-off curves of NO reduction and o-DCB oxidation over catalysts with different vanadium loading and under dry conditions are shown in Fig. 8A and 8B, respectively. Although NO and o-DCB conversions are presented in separate graphics, both reactions were carried out simultaneously.

In SCR reaction, NO conversion increases with temperature, up to 100%, in the region 100–300 °C, in which standard SCR reaction (Eq. (5)) is predominant. It should be noted total NO conversion is reached at lower temperature with high vanadium loading, being 230 °C for 3 $V/TiO_2$ and 8 $V/TiO_2$ and 310 °C for 1 $V/TiO_2$. However, at high temperature, NO conversion decreases because of the promotion of SCR side reactions, such as $NH_3$ oxidation (Eq. (6)) [60,61]. NO conversion drop takes place at higher temperature depending on the vanadium loading, at 328, 366 and 390 °C for 8 $V/TiO_2$, 3 $V/TiO_2$ and 1 $V/TiO_2$, respectively. Since oxidation reactions are involved in NO conversion drop at high temperature, this result suggests an improvement in oxidizing properties at higher vanadium loading.

On the other hand, o-DCB oxidation light-off curves show the typical S-shape. Below 200 °C, o-DCB conversion is extremely low. The increase of reaction temperature, between 200 and 250 °C, firstly promotes a moderate increase of o-DCB conversion. Then, o-DCB conversion sharply increases between 275 and 300 °C for 3 $V/TiO_2$ and 8 $V/TiO_2$, and between 320 and 400 °C for 1 $V/TiO_2$. So, in this temperature range, higher vanadium loading promotes a shift of o-DCB conversion curves towards lower temperatures. This result evidences the better oxidizing properties of high vanadium loading catalysts. Finally, at higher temperatures, o-DCB conversion increases slowly with temperature up to 100%. It is remarkable the distinct small plateau of 1 $V/TiO_2$ at temperatures between 250 and 300 °C (just below the light-off temperature).

$$4NO + 4NH_3 + O_2 \rightarrow 4\,N_2 + 6H_2O \quad (5)$$

$$4NH_3 + 5O_2 \rightarrow 4NO + 6H_2O \quad (6)$$

$$C_6H_4Cl_2 + O_2 \rightarrow 6CO_2 + H_2O + 2HCl \quad (7)$$

Fig. 8 has evidenced catalytic activity, for both NO reduction and o-DCB oxidation, is affected by vanadium dispersion, that is, by the vanadium species. In $VO_X/TiO_2$ catalysts, it is well known there are three functional groups depending on vanadium coverage, V = O, V-O-V and V-O-Ti [15]. Raman results showed V = O bonds in all catalysts, independently of vanadium loading; whereas V-O-V bonds were characteristic of polymeric and crystalline species. On the other hand, V-O-Ti

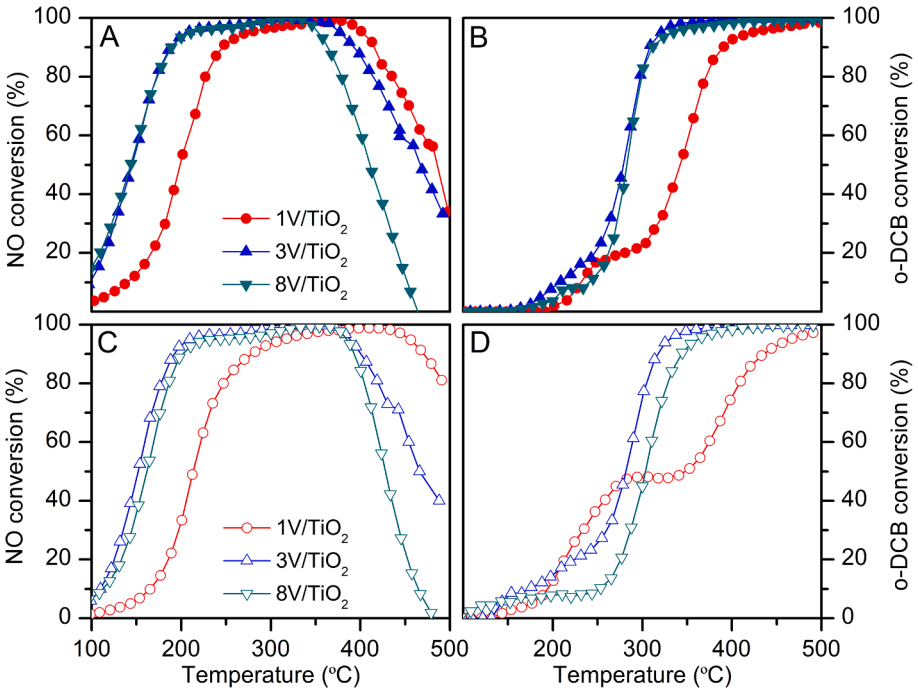


**Fig. 8.** Catalytic performances of $VO_X/TiO_2$ catalysts in the simultaneous SCR: A) under dry, and C) under wet conditions; and o-DCB oxidation: B) under dry, and D) under wet conditions (100 ppm o-DCB, 300 ppm NO, 300 ppm $NH_3$, 10% $O_2$, 0.5% $H_2O$, 2 $L_N$ $min^{-1}$, 1.5 atm and 80 $L_N$ (h g)$^{-1}$).

bonds only appear in isolated highly dispersed vanadium species. Since high vanadium-coverage catalysts (3 $V/TiO_2$ and 8 $V/TiO_2$) showed the higher NO and o-DCB conversion at lower temperatures; V-O-V bonds seems to play a key role in both SCR and o-DCB oxidation.

The better catalytic performances of high V-O-V bonds in SCR are associated to the higher mobility of lattice oxygen, which promotes the faster NO reduction by $NH_3$ and the catalytic surface reoxidation [57]. Nevertheless, the faster reoxidation of catalytic surface also promotes the easier oxidation of reagents involved in SCR. Therefore, this is the reason why higher vanadium loading also promotes a NO conversion drop at higher temperatures, as it was described above.

Moreover, acidity also plays an important role in SCR because it is involved in the reagents adsorption. According to TPD results, the increase of vanadium loading above 3% wt. promoted the loss of strong acidity. Only weak and medium acid strength were observed for high vanadium loading catalysts. As stated above, the increase of vanadium loading means the contribution of V-O-V bonds to V-O-Ti. Since 3 $V/TiO_2$ and 8 $V/TiO_2$ catalysts showed the higher NO conversion at low temperatures, the good catalytic performances of these catalysts in SCR are closely related to the medium and weak acidity provided by V-O-V bonds. This result is in accordance with some authors, who relate catalytic activity of low-temperature SCR reaction to weak acidity, usually linked to Brønsted acid sites provided by polymeric vanadium species [42,62].

In o-DCB oxidation, the good catalytic performances at low temperature of higher vanadium loading catalyst are associated to the faster oxygen dissociative chemisorption, provided by the high oxygen mobility, and the faster catalytic surface reoxidation. Both are key features to perform the oxidation reaction of adsorbed compounds. It should be noted catalytic activity increases significantly by increasing vanadium content from 1 to 3 wt%. Nevertheless, no improvement of o-DCB conversion occurs with the further increase from 3 to 8 wt%. Acordingly, Schimmoeller et al [37] concluded V-O-V bonds highly interacting with support are the most active species in chlorobenzene oxidation. Similar result was observed by Albonetti et al. [40], who reported 5.5 V atoms/$nm^2$ as the surface vanadium density from which o-DCB conversion does not further increase and associated this behavior to the activation of the aromatic molecule, promoted by Brønsted acidity, characteristic of polymeric species.

### 3.3. Catalytic performance in the presence of water

Fig. 8C and 8D show the light-off curves of NO and o-DCB obtained from the simultaneous abatement of NO and o-DCB in the presence of 0.5% of water vapor in the feedstream. Figs. 9 and 10 show the simultaneous NO and o-DCB conversion vs. TOS, in experiments of dry-wet-dry cycles over the three catalysts (1 $V/TiO_2$, 3 $V/TiO_2$ and 8 $V/TiO_2$) at three temperatures. In the wet stage, two concentrations of water, 0.5 and 2%, were used. Selection of the temperatures was made on the basis of the results obtained in the light-off experiments. The lowest temperature, 150 °C, was chosen because SCR reaction is predominant and the interference with parallel reactions is negligible. At this temperature, o-DCB oxidation rate is extremely low. The highest temperature, 350 °C, was chosen because o-DCB conversion is around or even slightly higher than 50%. At this temperature, NO reaction rate is considerably high, with a conversion level close to 100%, but the rate of $NH_3$ oxidation is also significant. The intermediate temperature, 250 °C, was chosen because o-DCB conversion is below 50%.

Both light-off curves and conversion-TOS curves show promoting and inhibiting effects of water on NO and o-DCB conversion depending on catalyst composition and temperature region.

#### 3.3.1. Effect of water on NO SCR

The light-off curves of SCR reaction (Fig. 8C) show that NO conversion is slightly lower in the presence of water below 300 °C, especially over 1 $V/TiO_2$ and 8 $V/TiO_2$. Around 375 °C, temperature at which side reactions are competing with NO reduction, the effect of water is the opposite: NO conversion increases with respect to dry conditions, especially over 1 $V/TiO_2$ and slightly over 8 $V/TiO_2$, while this does not significantly change in 3 $V/TiO_2$ catalyst.

NO conversions in Fig. 9 are not coincident with those in Fig. 8, since the transient response of light-off experiments is affected by catalyst thermal inertia. However, general behaviors are comparable. NO conversion at 150 °C is the lowest over 1 $V/TiO_2$ followed by 8 $V/TiO_2$ and

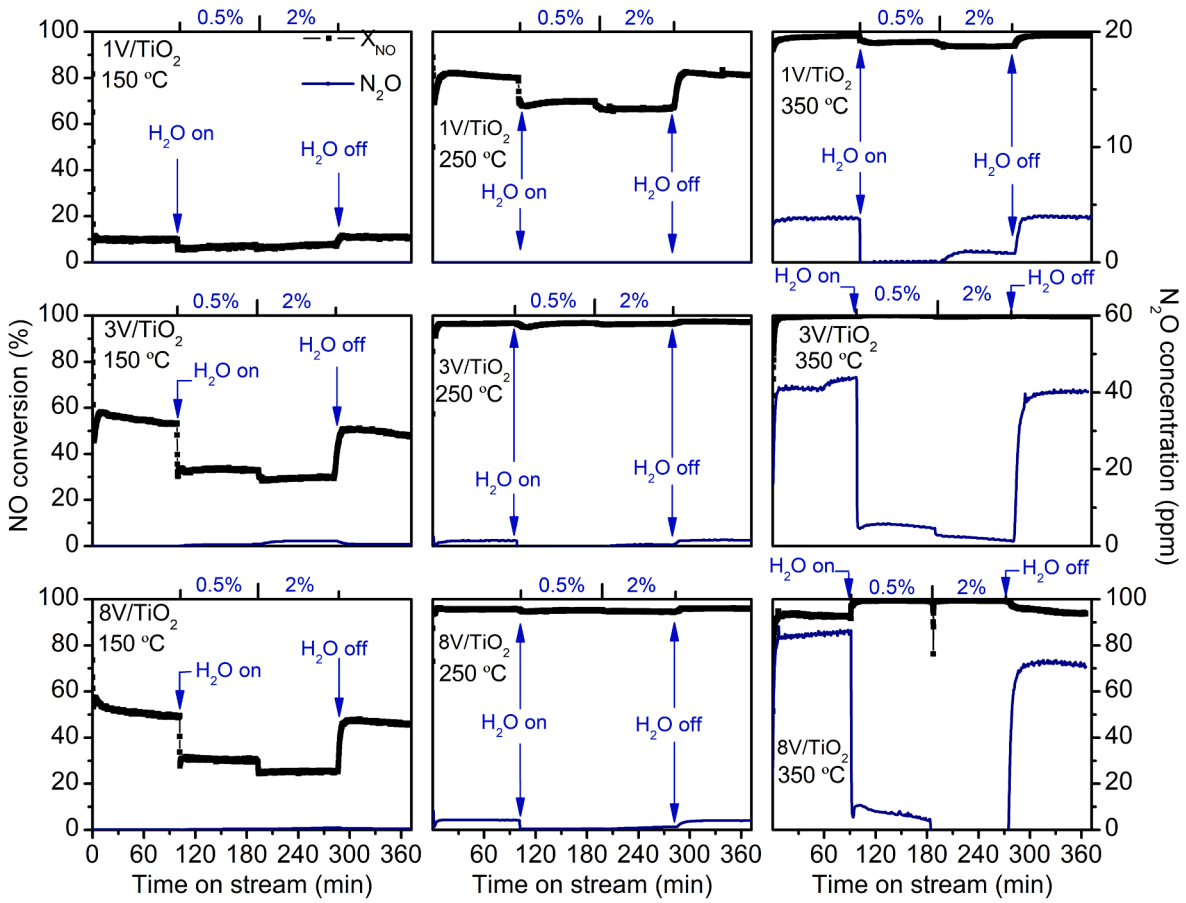


**Fig. 9.** Catalytic results in SCR reaction of dry/0.5%$H_2O$/2%$H_2O$/dry cycles for $VO_X/TiO_2$ catalysts (1 $V/TiO_2$ first row graphs, 3 $V/TiO_2$ second row graphs and 8 $V/TiO_2$ third row graphs) at different temperatures (150 °C first column graphs, 250 °C second column graphs and 350 °C third column graphs).

3 $V/TiO_2$. But, unlike light-off experiments, TOS experiments show weak signs of catalyst deactivation, since NO conversion decreases in the first 100 min TOS (dry conditions) from 58 to 53% in the case of 3 $V/TiO_2$ and from 57 to 49% in the case of 8 $V/TiO_2$. This issue will be discussed below.

Immediately after water concentration is increased from 0 to 0.5% (TOS = 100 min), NO conversion decreases, especially in the light-off region (conversion between 30 and 80%). For 1 $V/TiO_2$ at 250 °C, NO conversion decreases from 78 to 69%; for 3 $V/TiO_2$ at 150 °C, conversion decreases from 53 to 35%; and for 8 $V/TiO_2$ at 150 °C conversion decreases from 49 to 29%. Moreover, NO conversion further decreases when water concentration increases to 2% (TOS = 195 min), although to a lower extent than in the previous step, probably because of the high concentration of water compared to NO and $NH_3$. At the highest temperature, where conversion is near 100%, the effect of water is indiscernible. In the final step of the experiment, in which water is removed from the feedstream (TOS = 280 min), NO conversion increases to the initial level which suggests the inhibiting effect of water is reversible in SCR reaction. These results are consistent with those of other researchers who studied SCR inhibition by water over $V_2O_5/TiO_2$ catalysts. Amiridis et al. [34] quantified that water decreases the SCR TOF by approximately 40% at 350 °C. Huang et al. observed an increase of inhibiting effect as water concentration was increased at 250 °C [38].

The main hypothesis to explain the detrimental effect of water on NO conversion is a competition between water and reactants (NO and $NH_3$) involved in SCR reaction, as reported in the literature [38]. In order to verify this hypothesis, temperature programed desorption experiments of NO and $NH_3$ in dry and wet conditions were performed. These experiments were carried out in the above-described experimental setup, by online transferring reactor outlet gas stream to a mass selective spectrometer. Fig. 11 shows the profiles obtained from monitoring *m/z* 30 (NO) and 16 ($NH_3$). *m/z* 17 signal was not used for monitoring ammonia desorption because of the presence of significant interferences from desorbed water. NO and $NH_3$ desorption in dry conditions is higher than in wet conditions, as can be seen in the range 500–1500 s and above 2800 s and in the range 300–4200 s, respectively. These results confirm that both NO and $NH_3$ were adsorbed to a lower extent due to their competition with water for the same active sites. Such competition is also evidenced in the light-off curves (Fig. 8), by the higher NO conversion in the presence than in the absence of water at temperatures above 375 °C. Since $NH_3$ is competing with water for adsorption, $NH_3$ oxidation is inhibited, which leads to higher NO conversion. Furthermore, the effect of water is stronger over 1 $V/TiO_2$, followed by 8 $V/TiO_2$ and 3 $V/TiO_2$, as in the low-temperature region in which SCR reaction was predominant. Then, the effect of water is stronger over the less-active highly-dispersed monomeric species (1 $V/TiO_2$).

The effect of water on side reactions, such as nonselective catalytic reduction (NSCR) (Eq. (8)) and $NH_3$ catalytic oxidation (Eq. (9)) was also measured by monitoring the $N_2O$ concentration at the reactor outlet (Fig. 9, blue line). $N_2O$ is now considered as a pollutant due to its greenhouse effect and its depletion of the ozone layer [63]. On the one hand, $N_2O$ formation is not observed at low and medium temperature (150 and 250 °C), but it is remarkable at high temperature (350 °C). On the other hand, $N_2O$ production is notably high over highly loaded vanadium catalysts, like 8 $V/TiO_2$, composed mainly of crystalline species, followed by 3 $V/TiO_2$, composed mainly of highly polymerized species. This fact is in accordance with the sharper decay of NO conversion above 375 °C shown in Fig. 8A, and it is in line with the higher activity of highly polymerized and crystalline species compared to dispersed monomeric species in $NH_3$ oxidation. Yates et al. [64] also observed that

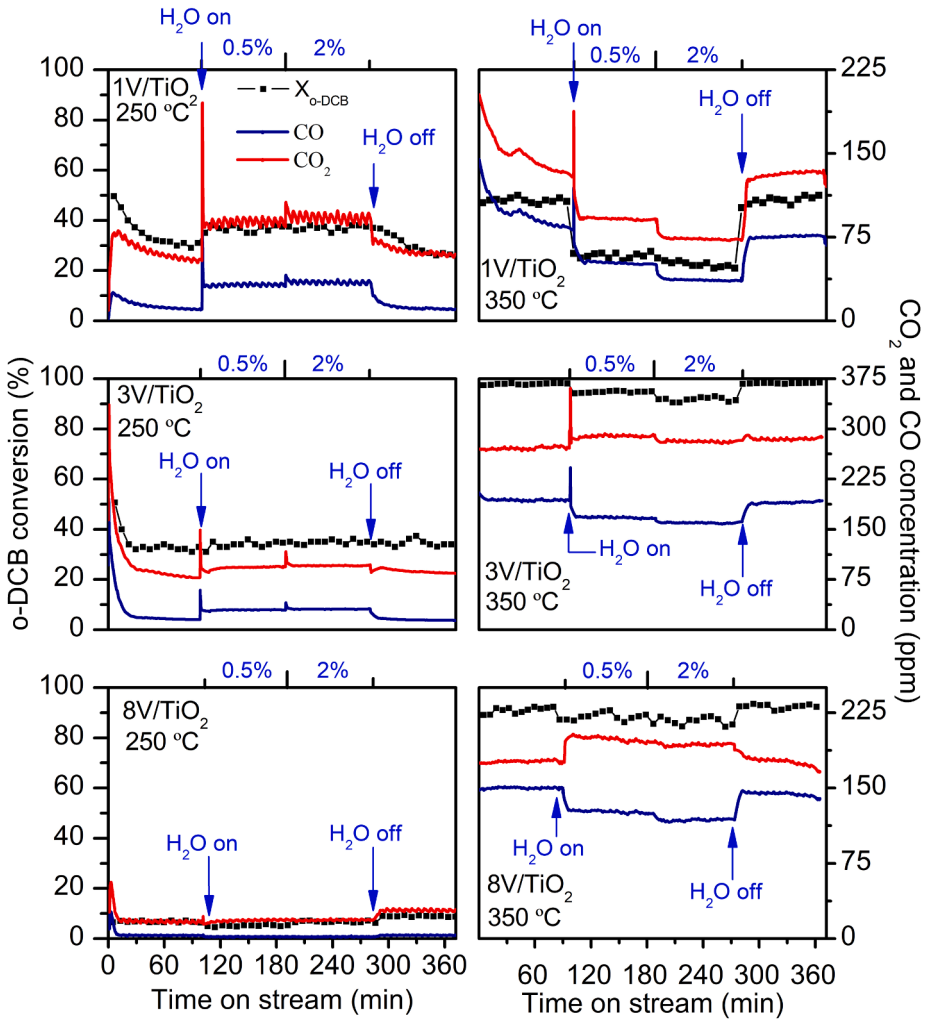


**Fig. 10.** Catalytic results in o-DCB oxidation reaction of dry/0.5%$H_2O$/2%$H_2O$/dry cycles for $VO_x/TiO_2$ catalysts (1 $V/TiO_2$ first row graphs, 3 $V/TiO_2$ second row graphs and 8 $V/TiO_2$ third row graphs) at different temperatures (150 °C first column graphs, 250 °C second column graphs and 350 °C third column graphs).

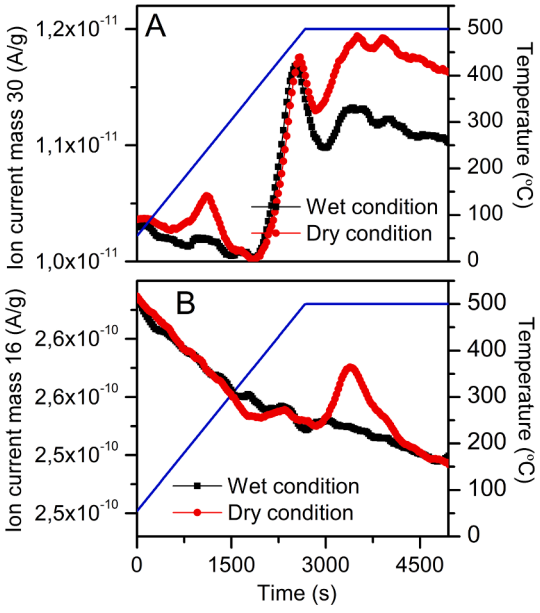


**Fig. 11.** Temperature programed desorption of NO (A) and $NH_3$ (B) under wet and dry condition.

selectivity to nitrogen, obtained during ammonia conversion experiments, fell abruptly for samples with high vanadium content above 240 °C, while the selectivity to $N_2O$ increased sharply.

$$4NH_3 + 4NO + 3O_2 \rightarrow 4N_2O + 6H_2O \quad (8)$$

$$2NH_3 + 2O_2 \rightarrow N_2O + 3H_2O \quad (9)$$

In this sense, Fig. 9 shows a decrease of $N_2O$ concentration from 43 to 6 ppm with 3 $V/TiO_2$ catalyst and from 86 to 7 ppm with 8 $V/TiO_2$ catalysts, when 0.5% water was introduced into the reactor. So, in presence of water, $N_2O$ production is inhibited and thus selectivity to $N_2$ is improved. Some authors also reported that water addition reduces $N_2O$ formation by suppressing $NH_3$ oxidation [65]. Moreover, Xiong et al. [66], who correlated the contribution of NSCR and $NH_3$ oxidation to $NH_3$ conversion under dry and wet conditions over $5V_2O_5$-$WO_3/TiO_2$ catalyst, they found the presence of water inhibited both reactions, leading to lower production of $N_2O$. Finally, when water concentration was increased to 2%, $N_2O$ formation drops even further, but to a much smaller proportion.

### 3.3.2. *Effect of water on o-DCB oxidation*

Light-off curves of o-DCB oxidation in Fig. 9D show that the effect of water is promoting at low temperature and inhibiting at high temperature. Below light-off temperature, o-DCB conversion is higher in the presence of water. In this sense, at 200 °C, o-DCB conversions are 12, 15

and 8% under wet conditions, whereas they are 2, 10 and 4% in the absence of water for 1 V/$TiO_2$, 3 V/$TiO_2$ and 8 V/$TiO_2$ catalysts, respectively. However, at high temperature, water clearly inhibits o-DCB conversion. The temperature for 90% conversion ($T_{90}$) increases from 390, 309 and 308 °C in the absence of water, to 434, 318 and 344 °C in the presence of water for 1 V/$TiO_2$, 3 V/$TiO_2$ and 8 V/$TiO_2$, respectively. 1 V/$TiO_2$ catalyst, in which isolated vanadium species are predominant, is the most affected by the presence of water both at low (promotion) and high (inhibition) temperature.

These two effects can also be observed in the conversion-TOS curves. Fig. 10 also collects the outlet CO and $CO_2$ concentrations vs. TOS for the dry-wet-dry cycle experiments. At 150 °C, o-DCB conversion is extremely low to appreciate a significant effect of water, and the results are not shown. At 250 °C, o-DCB conversion continuously decreases in the first 100 min in dry conditions: from 49 to 30% and from 50 to 31% for 1 V/$TiO_2$ and 3 V/$TiO_2$ catalysts, respectively. This is most probably due to catalyst deactivation, which also affects NO reduction but to a lower extent. In the case of 8 V/$TiO_2$, o-DCB conversion is so low that the deactivation is not noticeable. The decrease of o-DCB conversion goes with a decrease of CO and $CO_2$ production, evidencing that a lower amount of o-DCB is being oxidized with TOS. When water is introduced (0.5%) at 250 °C, o-DCB conversion and CO and $CO_2$ concentrations increase significantly for 1 V/$TiO_2$ and slightly for 3 V/$TiO_2$ with respect to conversion and concentration levels registered just before water addition. Furthermore, conversion is stable with TOS in the presence of water. Then, it seems that the promoting effect of water is related with the suppression of deactivation. But, if comparison is made with respect to conversion at TOS near zero (fresh catalysts and in the absence of water), it can be concluded that water is acting as inhibitor at the same time, since o-DCB conversion is lower in the presence of 0.5% of water, even in the case of 8 V/$TiO_2$, although the difference is rather small. The further increase of water concentration up to 2% does not affect o-DCB conversion with respect to the presence of 0.5% of water.

The inhibiting effect of water is clearer at 350 °C. In this temperature, o-DCB conversion, which is stable (no deactivation is observed) with TOS for all the catalysts in dry conditions, decreases with the addition of 0.5% of water (most notably over 1 V/$TiO_2$), and decreases even more with the addition of 2% water. However, when water is removed from the feedstream, back to dry conditions, o-DCB conversion increases to the levels of the previous dry step, also at 250 °C, which indicates that the effect of water in o-DCB oxidation is reversible. CO and $CO_2$ concentrations also recover the same values as measured in the first dry period. Then, the most plausible explanation of the detrimental effect of water is associated to a competitive adsorption with o-DCB for the active sites. This is also corroborated with the inhibition of NO SCR, as shown in Fig. 8C and Fig. 9, since $NH_3$ also competes with o-DCB for some of the active sites [42]. The inhibiting effect of water on $VO_X/TiO_2$ catalysts has already been observed by other authors [31,40,67].

The promoting effect of water can be associated to two facts observed in Fig. 10. On the one hand, the presence of water can affect differently CO and $CO_2$ concentration profiles. For 1 V/$TiO_2$ catalyst, CO and $CO_2$ concentration decrease in line with o-DCB conversion. However, for 3 V/$TiO_2$ and 8 V/$TiO_2$ catalysts, CO concentration also decreases, but $CO_2$ concentration increases, most notably in 8 V/$TiO_2$. This behaviour can only be associated to an increase of selectivity toward o-DCB total oxidation. This is corroborated in Table 2, which summarizes the $CO_2$ selectivity of the catalysts under dry and wet conditions at 350 °C. For all catalysts, even for 1 V/$TiO_2$, selectivity to $CO_2$ is higher in the presence of water. Fig. 12 shows that water also inhibits the formation of other chlorinated aromatic hydrocarbons, namely 3-chloro-2,5-furanodione and 3,4-dichloro-2,5-furanodione, formed from o-DCB decomposition at 350 °C on 8 V/$TiO_2$ catalyst. No chlorinated by-products were detected with the other catalysts, which suggests that partial oxidation of o-DCB is related to highly polymeric and crystal vanadium species at high temperatures.

On the other hand, the promoting effect of water on o-DCB is also

**Table 2**
Carbon and chlorine (Simultaneous SCR and o-DCB) and chlorine (o-DCB independent oxidation) contents of used samples at 250 °C and $CO_2$ selectivity at 350 °C.

| Sample | Simultaneous SCR and o-DCB oxidation | | | | | | o-DCB oxidation |
|---|---|---|---|---|---|---|---|
| | C (wt.%) at 250 °C | | Cl (wt.%) at 250 °C | | $CO_2$ selectivity (%) at 350 °C | | Cl (wt.%) at 250 °C |
| | Dry | Wet | Dry | Wet | Dry | Wet | Dry |
| 1 V/$TiO_2$ | 1.6 | –[a] | –[a] | –[a] | 55 | 72 | 0.3 |
| 3 V/$TiO_2$ | 5.6 | –[a] | –[a] | –[a] | 55 | 61 | –[a] |
| 8 V/$TiO_2$ | –[a] | –[a] | –[a] | –[a] | 39 | 44 | –[b] |

[a] Not detected
[b] Not analysed

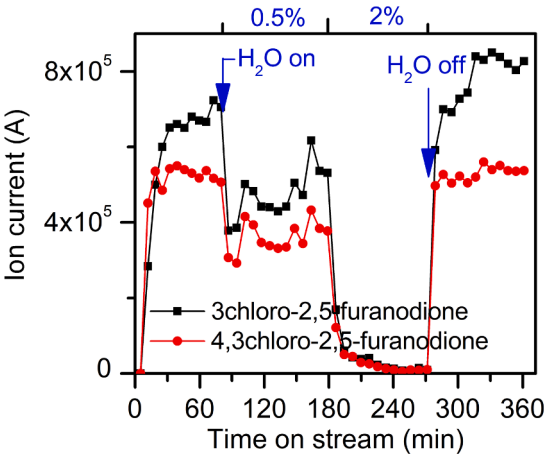


**Fig. 12.** Intensity of mass spectrum of chlorinated aromatic compounds detected by GC/MS during the experiment dry/0.5%$H_2O$/2%$H_2O$/dry cycle for 8 V/$TiO_2$ at 350 °C.

associated to the suppression of catalyst deactivation, since conversion of NO and o-DCB was kept constant with TOS for all catalysts and temperatures. The same behavior was observed when water concentration was increased to 2%. Concentration of outlet CO and $CO_2$ was also kept constant.

According to the literature, no deactivation of $VO_X/TiO_2$ for low temperature SCR is reported [49,68–70], but deactivation of catalysts in the oxidation of chlorinated hydrocarbons, due to the adsorption of detrimental species over the active sites, is widely reported [24,43,71–75]. Chlorine is one of the most referenced deactivating species for cerium oxide catalysts [76,77], supported noble-metal and metal catalysts [73], vanadium oxide based catalysts [44] and mixed metal catalysts [43]. Intermediate products formed in oxidation reactions are also important deactivating species in the oxidation of toluene over V/Ti-oxide and in the oxidation of trichloroethylene over Co and Cr oxide catalysts [78,79]. Finally, coke and carbonaceous species also cause deactivation in chlorinated hydrocarbon oxidation over zeolites and $VO_X/TiO_2$ catalysts [44,71].

However, the presence of water is reported as beneficial to prevent catalyst deactivation in the oxidation of chlorinated hydrocarbons. González-Velasco et al. [80] reported the removal of chlorine in the presence of water during the oxidation of chlorinated VOCs and Gallastegi-Villa et al. [74] corroborated the easier elimination of chlorine and coke in the presence of wet air compared to dry air. Hence, promotional effect of water over o-DCB conversion, observed at low temperature and low vanadium coverage, could be associated to the removal of deactivating species adsorbed on the surface of catalysts during reaction.

Table 2 summarizes carbon and chlorine contents of all catalysts

after the simultaneous NO reduction and o-DCB oxidation at 250 °C, both under dry and wet conditions. Under dry conditions, the catalysts in which deactivation was observed (1 V/$TiO_2$ and 3 V/$TiO_2$) present an important concentration of carbon of 1.6 and 5.6%, respectively. However, no relevant concentration of carbon was detected when the feedstream contained water (0.5%). These results reveal that water promotes fast removal (by hydrolysis) of surface carbonaceous species accumulated on the catalysts during the previous dry step, which causes the CO and $CO_2$ concentration peak just after water is introduced to the feedstream (Fig. 10).

Regarding to chlorine content on the catalyst surface, it was detected neither in dry nor wet conditions. The absence of chlorine is probably associated to the reaction between $NH_3$ and HCl or even surface chlorine ($Cl^-$) produced in o-DCB oxidation, to form $NH_4Cl$, which was detected on the particle filter located downstream the reactor. Hou et al. [81] also reported the formation of $NH_4Cl$ over $V_2O_5$/AC catalyst adding HCl to $NH_3$-SCR reaction mixture. In order to confirm this hypothesis, an independent o-DCB oxidation reaction was performed at 250 °C during 5 h for 1 V/$TiO_2$ and 3 V/$TiO_2$ catalysts. These samples underwent the most severe deactivation at conditions in Fig. 10. The surface analysis of both catalysts is shown in Table 2. The results confirm that chlorine accumulated over 1 V/$TiO_2$ catalysts up to 0.3 wt%, but no chlorine was detected over 3 V/$TiO_2$. These facts suggest that o-DCB oxidation occurs through the chlorine atoms, being more noticeable in the highly disperse vanadium catalysts [42]. However, increasing reaction temperature suppresses deactivation, due to absence of carbon and chlorine deposition as reported by several authors in the literature. Bertinchamps et al. [82], reported lower amount of carbon deposit and surface chlorine in toluene and chlorobenzene oxidation over $V_2O_5$/$TiO_2$ catalysts at high temperature. Gallastegi-Villa et al. [74] found that dry air to regenerate catalyst activity was more effective at higher temperature, since it aided both coke removal and chlorine removal, deposited in the oxidation of 1,2-dichloroethane and trichloroethylene over H-BEA zeolite.

Summing up, results reveal that water has a bimodal effect on o-DCB conversion, both positive and negative at the same time. The positive effect is associated to the removal of deactivating species adsorbed over the catalysts and promotion of complete oxidation of o-DCB to $CO_2$, whereas the negative effect is related to a competitive adsorption with o-DCB, and also with $NH_3$. The contribution of each effect depends on the vanadium species present on the surface of the catalyst and the temperature.

1 V/$TiO_2$ catalyst, composed mainly of isolated and some highly-disperse polymeric species, is strongly affected by deactivation at low temperature (250 °C), mainly caused by carbon species adsorbed on the catalyst surface. Thus, the contribution of water to the removal of deactivating species allows to increase o-DCB conversion (promoting effect) but not up to the values of the fresh catalyst (first minutes of TOS), since water also competes with o-DCB for the active sites (inhibiting effect).

At higher temperature (350 °C) deactivation is rather lower than at 250 °C. On the one hand, due to the higher oxidation rate of o-DCB and other intermediate by-products of incomplete oxidation; on the other hand, due to the lower adsorption of deactivating species. These two facts lead to lower amount of carbonaceous and chlorinated species deposited on the catalyst surface, as measured by the elemental analysis of carbon and chlorine. Then, at high temperature, the competitive adsorption between water and o-DCB becomes more relevant than the removal rate of deactivating species, whatever the catalyst composition (isolated, polymeric or crystalline species), although it is stronger over isolated monomeric species (1 V/$TiO_2$). As a result, the net effect of water is inhibiting, and leads to lower o-DCB conversion with respect to dry conditions.

These results are also consistent with the light-off curves. At low temperature, conversion of o-DCB is higher in the presence than in the absence of water, due to the high relevance of catalyst deactivation in dry conditions. Then, water contribution to the removal of deactivating species from the catalyst surface is higher than its competitive adsorption. This fact is more relevant over 1 V/$TiO_2$ (isolated monomeric species), followed by 3 V/$TiO_2$ (polymeric species) and 8 V/$TiO_2$ (crystalline species). At high temperature, conversion of o-DCB is lower in the presence than in the absence of water, due to the lower or irrelevant catalyst deactivation. Then, the competition between water and o-DCB for adsorption sites leads to lower conversion. This effect is also more relevant over 1 V/$TiO_2$, followed by 3 V/$TiO_2$ and 8 V/$TiO_2$.

## 4. Conclusions

$VO_X$/$TiO_2$ catalysts were prepared in order to study the influence of vanadium species in the effect of water on the simultaneous NO reduction through $NH_3$-SCR and o-DCB oxidation. Characterization results confirmed the presence of different vanadium species depending on vanadium loading. 1 V/$TiO_2$ catalysts showed highly dispersed or isolated vanadium species, and the increase of vanadium loading promotes the formation of polymeric species, in 3 V/$TiO_2$, and crystalline species, in 8 V/$TiO_2$, when the vanadium loading is above the monolayer. Catalytic tests showed that polymeric and crystalline species are the most active species, leading to high conversion of NO and o-DCB (higher than 80%) at low temperatures (above 200 °C). The effect of water is reversible in both reactions and depends on several factors. In SCR, water has a detrimental effect at low temperature because of competitive adsorption with the reactants involved in the reaction. However, at high temperature, water promotes NO conversion because of the inhibition of side reactions, which decreases the selectivity to $N_2O$ as well. Regarding to o-DCB oxidation, water has a bimodal effect, acting as both promotor, through the removal of detrimental species adsorbed over the catalysts, and inhibitor, due to a competitive adsorption with o-DCB. Thus, at low temperature and low vanadium coverages, with isolated and dispersed polymeric species, water promotes an increase of o-DCB conversion because the effect of removing adsorbed deactivating species (mainly carbonaceous) is stronger than competitive adsorption. On the other hand, at high temperature, where deactivation is lower, competitive adsorption of water leads to an inhibition of o-DCB conversion which is independent of vanadium species present on the catalysts. Moreover, water favors total oxidation of o-DCB to $CO_2$ and decreases the chlorinated by-products formed at high temperature.

## Declaration of Competing Interest

The authors declare that they have no known competing financial interests or personal relationships that could have appeared to influence the work reported in this paper.

## Acknowledgments

Authors thank MINECO/FEDER (CTQ2015-64616-P), MINECO (PID2019-107503RB-I00), Basque Government (IT657-13 and IT1297-19) and The University of the Basque Country, UPV/EHU (INF12/37, UFI 11/39) for the economic support. JAMM specially acknowledges MINECO/FEDER (BES-2016-077849) for the PhD grant. Likewise, the authors thank technical and human support provided by SGIker of UPV/EHU and European funding (ERDF and ESF).

## References

[1] G. McKay, Dioxin characterisation, formation and minimisation during municipal solid waste (MSW) incineration: Review, Chem. Eng. J. 86 (3) (2002) 343–368, https://doi.org/10.1016/S1385-8947(01)00228-5.

[2] J. Kuo, H. Tseng, P.S. Rao, M. Wey, The prospect and development of incinerators for municipal solid waste treatment and characteristics of their pollutants in Taiwan, Appl. Therm. Eng. 28 (2008) 2305–2314, https://doi.org/10.1016/j.applthermaleng.2008.01.010.

[3] M. Wey, W. Ou, Z. Liu, H. Tseng, W. Yang, B. Chiang, Pollutants in incineration flue gas, J. Hazard. Mater. 82 (2001) 247–262, https://doi.org/10.1016/S0304-3894(00)00355-1.

[4] I. Hwang, H. Minoya, T. Matsuto, T. Matsuo, A. Matsumoto, R. Sameshima, Removal of ammonium chloride generated by ammonia slip from the SNCR process in municipal solid waste incinerators, Chemosphere 74 (2009) 1379–1384, https://doi.org/10.1016/j.chemosphere.2008.11.008.

[5] J. De Greef, K. Villani, J. Goethals, H. Van Belle, J. Van Caneghem, C. Vandecasteele, Optimising energy recovery and use of chemicals, resources and materials in modern waste-to-energy plants, Waste Manage. 33 (11) (2013) 2416–2424, https://doi.org/10.1016/j.wasman.2013.05.026.

[6] O. Gohlke, T. Weber, P. Seguin, Y. Laborel, A new process for $NO_X$ reduction in combustion systems for the generation of energy from waste, Waste Manage. 30 (7) (2010) 1348–1354, https://doi.org/10.1016/j.wasman.2010.02.024.

[7] G. Wielgosiński, J. Czerwińska, O. Szymańska, J. Bujak, Simultaneous $NO_X$ and dioxin removal in the SNCR process, Sustainability 12 (2020) 1–10, https://doi.org/10.3390/su12145766.

[8] M. Tayyeb Javed, N. Irfan, B.M. Gibbs, Control of combustion-generated nitrogen oxides by selective non-catalytic reduction, J. Environ. Manage. 83 (3) (2007) 251–289, https://doi.org/10.1016/j.jenvman.2006.03.006.

[9] J. Van Caneghem, J. De Greef, C. Block, C. Vandecasteele, $NO_X$ reduction in waste incinerators by selective catalytic reduction (SCR) instead of selective non catalytic reduction (SNCR) compared from a life cycle perspective: A case study, J. Clean. Prod. 112 (2016) 4452–4460, https://doi.org/10.1016/j.jclepro.2015.08.068.

[10] F. Neuwahl, G. Cusano, J. Gómez Benavides, S. Holbrook, S. Roudier, Best Available Techniques (BAT) Reference Document for Waste Incineration; EUR 29971 EN; doi:10.2760/761437.

[11] K. Villani, J. De Greef, J. Goethals, I. Montauban, H. Van Langenhove, Exploring the performance limits of non-catalytic de-NOX in waste-to-energy-plants. In: Proceedings Venice 2012, 4th International Symposium on Energy from Biomass and Waste. CISA publisher, Italy.

[12] K. Skalska, J.S. Miller, S. Ledakowicz, Trends in $NO_X$ abatement: A review, Sci. Total Environ. 408 (19) (2010) 3976–3989, https://doi.org/10.1016/j.scitotenv.2010.06.001.

[13] M.A. Gómez-García, V. Pitchon, A. Kiennemann, Pollution by nitrogen oxides: An approach to $NO_X$ abatement by using sorbing catalytic materials, Environ. Int. 31 (2005) 445–467, https://doi.org/10.1016/j.envint.2004.09.006.

[14] E. FINOCCHIO, G. BUSCA, M. NOTARO, A review of catalytic processes for the destruction of PCDD and PCDF from waste gases, Appl. Catal. B Environ. 62 (1-2) (2006) 12–20, https://doi.org/10.1016/j.apcatb.2005.06.010.

[15] C. Du, S. Lu, Q. Wang, A.G. Buekens, M. Ni, D.P. Debecker, A review on catalytic oxidation of chloroaromatics from flue gas, Chem. Eng. J 334 (2018) 519–544, https://doi.org/10.1016/j.cej.2017.09.018.

[16] Y. Peng, J. Chen, S. Lu, J. Huang, M. Zhang, A. Buekens, X. Li, J. Yan, Chlorophenols in Municipal Solid Waste Incineration: A review, Chem. Eng. J 292 (2016) 398–414, https://doi.org/10.1016/j.cej.2016.01.102.

[17] K. Everaert, J. Baeyens, Removal of PCDD/F from flue gases in fixed or moving bed adsorbers, Waste Manage. 24 (1) (2004) 37–42, https://doi.org/10.1016/S0956-053X(03)00136-3.

[18] A. Brasseur, A. Gambin, A. Laudet, J. Marien, J. Pirard, Elaboration of new formulations to remove micropollutants in MSWI flue gas, Chemosphere 56 (2004) 745–756, https://doi.org/10.1016/j.chemosphere.2004.04.049.

[19] H.J. Fell, M. Tuczek, Removal of dioxins and furans from flue gases by non-flammable adsorbents in a fixed bed, Chemosphere 37 (9-12) (1998) 2327–2334, https://doi.org/10.1016/S0045-6535(98)00291-4.

[20] P. Liljelind, J. Unsworth, O. Maaskant, S. Marklund, Removal of dioxins and related aromatic hydrocarbons from flue gas streams by adsorption and catalytic destruction, Chemosphere 42 (5-7) (2001) 615–623, https://doi.org/10.1016/S0045-6535(00)00235-6.

[21] J.L. Bonte, K.J. Fritsky, M.A. Plinke, M. Wilken, Catalytic destruction of PCDD/F in a fabric filter: Experience at a municipal waste incinerator in Belgium, Waste Manage. 22 (2002) 421–426, https://doi.org/10.1016/S0956-053X(02)00025-9.

[22] M. Syc, V. Pekárek, E. Fišerová, M. Punčochář, J. Karban, O. Prokeš, Catalytic filter application in the termizo municipal waste incineration plant in Liberec, Organohalogen Compounds 68 (2006) 1232–1235.

[23] P.C. Hung, S.H. Chang, M.B. Chang, Removal of chlorinated aromatic organic compounds from MWI with catalytic filtration, Aerosol Air Qual. Res. 14 (4) (2014) 1215–1222, https://doi.org/10.4209/aaqr.2013.02.0041.

[24] M.S. Kamal, S.A. Razzak, M.M. Hossain, Catalytic oxidation of volatile organic compounds (VOCs)-A review, Atmos. Environ. 140 (2016) 117–134, https://doi.org/10.1016/j.atmosenv.2016.05.031.

[25] M. Goemans, P. Clarysse, J. Joannès, P. De Clercq, S. Lenaerts, K. Matthys, K. Boels, Catalytic $NO_X$ reduction with simultaneous dioxin and furan oxidation, Chemosphere 54 (9) (2004) 1357–1365, https://doi.org/10.1016/S0045-6535(03)00255-8.

[26] J. Jones, J.R.H. Ross, The development of supported vanadia catalysts for the combined catalytic removal of the oxides of nitrogen and of chlorinated hydrocarbons from flue gases, Catal. Today 35 (1-2) (1997) 97–105, https://doi.org/10.1016/S0920-5861(96)00148-4.

[27] L.-C. Wang, W.-J. Lee, P.-J. Tsai, W.-S. Lee, G.-P. Chang-Chien, Emissions of polychlorinated dibenzo-p-dioxins and dibenzofurans from stack flue gases of sinter plants, Chemosphere 50 (9) (2003) 1123–1129, https://doi.org/10.1016/S0045-6535(02)00702-6.

[28] M. Goemans, P. Clarysse, J. Joannès, P. De Clercq, S. Lenaerts, K. Matthys, K. Boels, Catalytic $NO_X$ reduction with simultaneous dioxin and furan oxidation, Chemosphere 50 (4) (2003) 489–497, https://doi.org/10.1016/S0045-6535(02)00554-4.

[29] S. Lomnicki, J. Lichtenberger, Z. Xu, M. Waters, J. Kosman, M.D. Amiridis, Catalytic oxidation of 2,4,6-trichlorophenol over vanadia/titania-based catalysts, Appl. Catal. B Environ 46 (1) (2003) 105–119, https://doi.org/10.1016/S0926-3373(03)00215-7.

[30] J. Lichtenberger, M.D. Amiridis, Catalytic oxidation of chlorinated benzenes over $V_2O_5/TiO_2$ catalysts, J. Catal. 223 (2004) 296–308, https://doi.org/10.1016/j.jcat.2004.01.032.

[31] F. Bertinchamps, C. Grégoire, E.M. Gaigneaux, Systematic investigation of supported transition metal oxide based formulations for the catalytic oxidative elimination of (chloro)-aromatics: Part I: Identification of the optimal main active phases and supports, Appl. Catal. B Environ 66 (2006) 1–9, https://doi.org/10.1016/j.apcatb.2006.02.011.

[32] R. Weber, T. Sakurai, H. Hagenmaier, Low temperature decomposition of PCDD/PCDF, chlorobenzenes and PAHs by TiO2-based $V_2O_5$-$WO_3$ catalysts, Appl. Catal. B Environ. 20 (1999) 249–256, https://doi.org/10.1016/S0926-3373(98)00115-5.

[33] J.-K. Lai, I.E. Wachs, A Perspective on the Selective Catalytic Reduction (SCR) of NO with $NH_3$ by supported $V_2O_5$-$WO_3/TiO_2$ Catalysts, ACS Catalysis 8 (7) (2018) 6537–6551, https://doi.org/10.1021/acscatal.8b01357.

[34] M.D. Amiridis, I.E. Wachs, G. Deo, J. Jehng, D.S. Kim, Reactivity of $V_2O_5$ catalysts for the selective catalytic reduction of NO by $NH_3$: Influence of vanadia loading, $H_2O$, and $SO_2$, J. Catal. 161 (1996) 247–253, https://doi.org/10.1006/jcat.1996.0182.

[35] S. Krishnamoorthy, J.P. Baker, M.D. Amiridis, Catalytic oxidation of 1,2-dichlorobenzene over $V_2O_5/TiO_2$-based catalysts, Catal. Today 40 (1998) 39–46, https://doi.org/10.1016/S0920-5861(97)00117-X.

[36] R. Delaigle, D.P. Debecker, F. Bertinchamps, E.M. Gaigneaux, Revisiting the behaviour of vanadia-based catalysts in the abatement of (chloro)-aromatic pollutants: Towards an integrated understanding, Top Catal 52 (2009) 501–516, https://doi.org/10.1007/s11244-009-9181-9.

[37] B. Schimmoeller, R. Delaigle, D.P. Debecker, E.M. Gaigneaux, Flame-made vs. wet-impregnated vanadia/titania in the total oxidation of chlorobenzene: Possible role of $VO_X$ species, Catal Today 157 (2010) 198–203, https://doi.org/10.1016/j.cattod.2010.01.029.

[38] Z. Huang, Z. Liu, X. Zhang, Q. Liu, Inhibition effect of $H_2O$ on $V_2O_5$/AC catalyst for catalytic reduction of NO with $NH_3$ at low temperature, Appl. Catal. B Environ 63 (3-4) (2006) 260–265, https://doi.org/10.1016/j.apcatb.2005.10.011.

[39] K. Poplawski, J. Lichtenberger, F.J. Keil, K. Schnitzlein, M.D. Amiridis, Catalytic oxidation of 1,2-dichlorobenzene over $ABO_3$-type perovskites, Catal. Today 62 (4) (2000) 329–336, https://doi.org/10.1016/S0920-5861(00)00434-X.

[40] S. Albonetti, S. Blasioli, R. Bonelli, J.E. Mengou, S. Scirè, F. Trifirò, The role of acidity in the decomposition of 1,2-dichlorobenzene over $TiO_2$-based $V_2O_5/WO_3$ catalysts, Appl Catal A Gen 341 (1-2) (2008) 18–25, https://doi.org/10.1016/j.apcata.2007.12.033.

[41] M. Gallastegi-Villa, A. Aranzabal, Z. Boukha, J.A. González-Marcos, J.R. González-Velasco, M.V. Martínez-Huerta, M.A. Bañares, Role of surface vanadium oxide coverage support on titania for the simultaneous removal of o-dichlorobenzene and $NO_X$ from waste incinerator flue gas, Catal Today 254 (2015) 2–11, https://doi.org/10.1016/j.cattod.2015.02.029.

[42] M. Gallastegi-Villa, A. Aranzabal, M.P. González-Marcos, B. Markaide-Aiastui, J. A. González-Marcos, J.R. GonzÃ¡lez-Velasco, Effect of vanadia loading on acidic and redox properties of $VO_X/TiO_2$ for the simultaneous abatement of PCDD/Fs and $NO_X$, J Ind Eng Chem 81 (2020) 440–450, https://doi.org/10.1016/j.jiec.2019.09.034.

[43] J.A. Martín-Martín, J. Sánchez-Robles, M.P. González-Marcos, A. Aranzabal, J. R. González-Velasco, Effect of preparation procedure and composition of catalysts based on Mn and Ce oxides in the simultaneous removal of $NO_X$ and o-DCB, Mol. Cat. 495 (2020), https://doi.org/10.1016/j.mcat.2020.111152.

[44] C.E. Hetrick, F. Patcas, M.D. Amiridis, Effect of water on the oxidation of dichlorobenzene over $V_2O_5/TiO_2$ catalysts, Appl. Catal. B Environ. 101 (3-4) (2011) 622–628, https://doi.org/10.1016/j.apcatb.2010.11.003.

[45] C.-H. Cho, S.-K. Ihm, Development of new vanadium-based oxide catalysts for decomposition of chlorinated aromatic pollutants, Environ. Sci. and Technol. 36 (7) (2002) 1600–1606, https://doi.org/10.1021/es015687h.

[46] I.E. Wachs, B.M. Weckhuysen, Structure and reactivity of surface vanadium oxide species on oxide supports, Appl Catal A: Gen 157 (1997) 67–90, https://doi.org/10.1016/S0926-860X(97)00021-5.

[47] J. Choi, C.B. Shin, T. Park, D.J. Suh, Characteristics of vanadia-titania aerogel catalysts for oxidative destruction of 1,2-dichlorobenzene, Appl Catal A Gen 311 (2006) 105–111, https://doi.org/10.1016/j.apcata.2006.06.030.

[48] M.A. Vuurman, I.E. Wachs, A.M. Hirt, Structural determination of supported $V_2O_5$-$WO_3/TiO_2$ catalysts by in situ Raman spectroscopy and X-ray photoelectron spectroscopy, J. Phys. Chem. 95 (1991) 9928–9937, https://doi.org/10.1021/j100177a059.

[49] I. Giakoumelou, C. Fountzoula, C. Kordulis, S. Boghosian, Molecular structure and catalytic activity of $V_2O_5/TiO_2$ catalysts for the SCR of NO by $NH_3$: In situ Raman spectra in the presence of $O_2$, $NH_3$, NO, $H_2$, $H_2O$, and $SO_2$, J. Catal. 239 (2006) 1–12, https://doi.org/10.1016/j.jcat.2006.01.019.

[50] M. Gallastegi-Villa, A. Aranzabal, J.A. González-Marcos, J.R. González-Velasco, Tailoring dual redox-acid functionalities in $VO_X/TiO_2$/ZSM5 catalyst for simultaneous abatement of PCDD/Fs and $NO_X$ from municipal solid waste incineration, Appl. Catal. B Environ. 205 (2017) 310–318, https://doi.org/10.1016/j.apcatb.2016.12.020.

[51] J. Wang, X. Wang, X. Liu, J. Zeng, Y. Guo, T. Zhu, Kinetics and mechanism study on catalytic oxidation of chlorobenzene over $V_2O_5/TiO_2$ catalysts, J Mol Catal A Chem 402 (2015) 1–9, https://doi.org/10.1016/j.molcata.2015.03.003.

[52] Q. Sun, Y. Fu, J. Liu, A. Auroux, J. Shen, Structural, acidic and redox properties of $V_2O_5$-$TiO_2$-$SO_4^{2-}$ catalysts, Appl Catal A Gen 334 (1-2) (2008) 26–34, https://doi.org/10.1016/j.apcata.2007.09.023.

[53] S. Besselmann, C. Freitag, O. Hinrichsen, M. Muhler, Temperature-programmed reduction and oxidation experiments with $V_2O_5/TiO_2$ catalysts, Phys. Chem. Chem. Phys. 3 (2001) 4633–4638, https://doi.org/10.1039/b105466j.
[54] J. Yang, Q. Yang, J. Sun, Q. Liu, D. Zhao, W. Gao, L. Liu, Effects of mercury oxidation on $V_2O_5$-$WO_3/TiO_2$ catalyst properties in $NH_3$-SCR process, Catal. Commun. 59 (2015) 78–82, https://doi.org/10.1016/j.catcom.2014.09.049.
[55] X. Zhao, Y. Yan, L. Mao, M. Fu, H. Zhao, L. Sun, Y. Xiao, G. Dong, A relationship between the $V^{4+}/V^{5+}$ ratio and the surface dispersion, surface acidity, and redox performance of $V_2O_5$-$WO_3/TiO_2$ SCR catalysts, RSC Adv. 8 (54) (2018) 31081–31093, https://doi.org/10.1039/C8RA02857E.
[56] S. Zhang, Q. Zhong, Surface characterization studies on the interaction of $V_2O_5$-$WO_3/TiO_2$ catalyst for low temperature SCR of NO with $NH_3$, J. Solid State Chem. 221 (2015) 49–56, https://doi.org/10.1016/j.jssc.2014.09.008.
[57] S. Youn, S. Jeong, D.H. Kim, Effect of oxidation states of vanadium precursor solution in $V_2O_5/TiO_2$ catalysts for low temperature $NH_3$ selective catalytic reduction, Catal Today 232 (2014) 185–191, https://doi.org/10.1016/j.cattod.2014.01.025.
[58] F. Tang, K. Zhuang, F. Yang, L. Yang, B. Xu, J. Qiu, Y. Fan, Effect of dispersion state and surface properties of supported vanadia on the activity of $V_2O/TiO_2$ catalysts for the selective catalytic reduction of NO by $NH_3$, Chinese J Catal 33 (2012) 933–940, https://doi.org/10.1016/S1872-2067(11)60365-3.
[59] G. Ramis, L. Yi, G. Busca, Ammonia activation over catalysts for the selective catalytic reduction of NOx and the selective catalytic oxidation of NH3, An FT-IR study, Catal Today 28 (4) (1996) 373–380, https://doi.org/10.1016/S0920-5861(96)00050-8.
[60] G. Madia, M. Koebel, M. Elsener, A. Wokaun, Side reactions in the selective catalytic reduction of $NO_X$ with various $NO_2$ fractions, Ind Eng Chem Res 41 (16) (2002) 4008–4015, https://doi.org/10.1021/ie020054c.
[61] M.H. Kim, S.-W. Ham, Determination of $N_2O$ emissions levels in the selective reduction of $NO_X$ by $NH_3$ over an on-site-used commercial $V_2O_5$-$WO_3/TiO_2$ catalyst using a modified gas cell, Top. Catal. 53 (7-10) (2010) 597–607, https://doi.org/10.1007/s11244-010-9493-9.
[62] C. Sun, L. Dong, W. Yu, L. Liu, H. Li, F. Gao, L. Dong, Y. Chen, Promotion effect of tungsten oxide on SCR of NO with $NH_3$ for the $V_2O_5$-$WO_3/Ti_{0.5}Sn_{0.5}O_2$ catalyst: Experiments combined with DFT calculations, J Mol Catal A: Chem 346 346 (1-2) (2011) 29–38, https://doi.org/10.1016/j.molcata.2011.06.004.
[63] D. Zhang, R.T. Yang, $N_2O$ Formation Pathways over Zeolite-Supported Cu and Fe Catalysts in $NH_3$-SCR, Energy Fuels 32 (2) (2018) 2170–2182, https://doi.org/10.1021/acs.energyfuels.7b0340510.1021/acs.energyfuels.7b03405.s001.
[64] M. Yates, J.A. Martín, M.A. Martín-Luengo, S. Suárez, J. Blanco, $N_2O$ formation in the ammonia oxidation and in the SCR process with $V_2O_5$-$WO_3$ catalysts, Catal Today 107–108 (2005) 120–125, https://doi.org/10.1016/j.cattod.2005.07.015.
[65] L.J. Alemany, L. Lietti, N. Ferlazzo, P. Forzatti, G. Busca, E. Giamello, F. Bregani, Reactivity and physicochemical characterization of $V_2O_5$-$WO_3/TiO_2$ De-NOx catalysts, J. Catal. 155 (1995) 117–130, https://doi.org/10.1006/jcat.1995.1193.
[66] S. Xiong, X. Xiao, Y. Liao, H. Dang, W. Shan, S. Yang, Global Kinetic Study of NO Reduction by $NH_3$ over $V_2O_5$-$WO_3/TiO_2$: Relationship between the SCR Performance and the Key Factors, Ind. Eng. Chem. Res. 54 (2015) 11011–11023, https://doi.org/10.1021/acs.iecr.5b03044.
[67] S. Krishnamoorthy, J.A. Rivas, M.D. Amiridis, Catalytic Oxidation of 1,2-Dichlorobenzene over Supported Transition Metal Oxides, J Catal 193 (2) (2000) 264–272, https://doi.org/10.1006/jcat.2000.2895.
[68] S.S.R. Putluru, L. Schill, A. Godiksen, R. Poreddy, S. Mossin, A.D. Jensen, R. Fehrmann, Promoted $V_2O_5/TiO_2$ catalysts for selective catalytic reduction of NO with $NH_3$ at low temperatures, Appl. Catal. B Environ. 183 (2016) 282–290, https://doi.org/10.1016/j.apcatb.2015.10.044.
[69] Y. He, M.E. Ford, M. Zhu, Q. Liu, U. Tumuluri, Z. Wu, I.E. Wachs, Influence of catalyst synthesis method on selective catalytic reduction (SCR) of NO by $NH_3$ with $V_2O_5$-$WO_3/TiO_2$ catalysts, Appl. Catal. B Environ. 193 (2016) 141–150, https://doi.org/10.1016/j.apcatb.2016.04.022.
[70] Z. Liu, S. Zhang, J. Li, J. Zhu, L. Ma, Novel $V_2O_5$-$CeO_2/TiO_2$ catalyst with low vanadium loading for the selective catalytic reduction of $NO_X$ by $NH_3$, Appl. Catal. B Environ 158–159 (2014) 11–19, https://doi.org/10.1016/j.apcatb.2014.03.049.
[71] A. Aranzabal, M. Romero-Sáez, U. Elizundia, J.R. González-Velasco, J.A. González-Marcos, Deactivation of H-zeolites during catalytic oxidation of trichloroethylene, J Catal 296 (2012) 165–174, https://doi.org/10.1016/j.jcat.2012.09.012.
[72] N. Abbas, M. Hussain, N. Russo, G. Saracco, Studies on the activity and deactivation of novel optimized $TiO_2$ nanoparticles for the abatement of VOCs, Chem. Eng. J. 175 (2011) 330–340, https://doi.org/10.1016/j.cej.2011.09.115.
[73] M. Guillemot, J. Mijoin, S. Mignard, P. Magnoux, Mode of zeolite catalysts deactivation during chlorinated VOCs oxidation, Appl Catal A Gen 327 (2) (2007) 211–217, https://doi.org/10.1016/j.apcata.2007.05.012.
[74] M. Gallastegi-Villa, A. Aranzabal, M. Romero-Sáez, J.A. González-Marcos, J. R. González-Velasco, Catalytic activity of regenerated catalyst after the oxidation of 1,2-dichloroethane and trichloroethylene, Chem. Eng. J. 241 (2014) 200–206, https://doi.org/10.1016/j.cej.2013.12.008.
[75] S. Ihm, Y. Jun, D. Kim, K. Jeong, Low-temperature deactivation and oxidation state of Pd/γ-$Al_2O_3$ catalysts for total oxidation of n-hexane, Catal. Today 93–95 (2004) 149–154, https://doi.org/10.1016/j.cattod.2004.06.096.
[76] Y. Dai, X. Wang, Q. Dai, D. Li, Effect of Ce and La on the structure and activity of $MnO_X$ catalyst in catalytic combustion of chlorobenzene, Appl. Catal. B Environ. 111–112 (2012) 141–149, https://doi.org/10.1016/j.apcatb.2011.09.028.
[77] W. Xingyi, K. Qian, L. Dao, Catalytic combustion of chlorobenzene over $MnO_X$-$CeO_2$ mixed oxide catalysts, Appl. Catal. B Environ. 86 (3-4) (2009) 166–175, https://doi.org/10.1016/j.apcatb.2008.08.009.
[78] L.C.A. Oliveira, R.M. Lago, J.D. Fabris, K. Sapag, Catalytic oxidation of aromatic VOCs with Cr or Pd-impregnated Al-pillared bentonite: Byproduct formation and deactivation studies, Appl. Clay. Sci. 39 (3-4) (2008) 218–222, https://doi.org/10.1016/j.clay.2007.06.003.
[79] D.A. Bulushev, S.I. Reshetnikov, L. Kiwi-Minsker, A. Renken, Deactivation kinetics of V/Ti-oxide in toluene partial oxidation, Appl Catal A Gen 220 (1-2) (2001) 31–39, https://doi.org/10.1016/S0926-860X(01)00701-3.
[80] J.R. González-Velasco, A. Aranzabal, R. López-Fonseca, R. Ferret, J.A. González-Marcos, Enhancement of the catalytic oxidation of hydrogen-lean chlorinated VOCs in the presence of hydrogen-supplying compounds, Appl. Catal. B Environ 24 (1) (2000) 33–43, https://doi.org/10.1016/S0926-3373(99)00087-9.
[81] Y. Hou, G. Cai, Z. Huang, X. Han, S. Guo, Effect of HCl on $V_2O_5$/AC catalyst for NO reduction by $NH_3$ at low temperatures, Chem. Eng. J. 247 (2014) 59–65, https://doi.org/10.1016/j.cej.2014.01.036.
[82] F. Bertinchamps, C. Poleunis, C. Grégoire, P. Eloy, P. Bertrand, E.M. Gaigneaux, Elucidation of deactivation or resistance mechanisms of $CrO_X$, $VO_X$ and $MnO_X$ supported phases in the total oxidation of chlorobenzene via ToF-SIMS and XPS analyses, Surf. Interface Anal. 40 (3-4) (2008) 231–236, https://doi.org/10.1002/(ISSN)1096-991810.1002/sia.v40:3/410.1002/sia.2627.